ings have been characterized as a function of depth at the primary cross-linking site by using the complementary techniques of diffuse reflectance infrared spectroscopy and solid-state ^{13}C NMR. The curing of an acid-catalyzed coating is shown to go to completion with respect to acrylic hydroxyl under the conditions used, with no significant concurrent melamine self-condensation reactions. Degradation is promoted by the presence of heat and/or light, residual acid, and atmospheric water; the degradative pathway invokes irreversible acid-catalyzed hydrolysis of residual $>NCH_2OCH_3$ throughout the coating and primary cross-links only at the very surface.

Acknowledgment. We gratefully acknowledge the skilled technical assistance of Dr. R. D. Farlee and Mr. R. H. Kern.

Registry No. CBT, 3071-66-7; methyl methacrylate–butyl acrylate–hydroxyethyl acrylate copolymer, 25951-38-6; *n*-propylamine, 107-10-8; cyanuric chloride, 108-77-0.

References and Notes

(1) D. R. Bauer and R. A. Dickie, *J. Polym. Sci., Polym. Phys. Ed.*, 18, 1997 (1980).
(2) D. R. Bauer and R. A. Dickie, *J. Polym. Sci., Polym. Phys. Ed.*, 18, 2015 (1980).
(3) W. J. Blank, *J. Coat. Technol.*, 51 (656), 61 (1979).
(4) D. R. Bauer, *J. Appl. Polym. Sci.*, 27, 3651 (1982).
(5) M. P. Fuller and P. R. Griffiths, *Anal. Chem.*, 50, 1906 (1978).
(6) R. H. Norton and R. J. Beer, *J. Opt. Soc. Am.*, 66, 259 (1976).
(7) E. O. Stejskal and J. Schaefer, *J. Magn. Reson.* 18, 560 (1975).
(8) J. W. Beams, *Rev. Sci. Instrum.*, 1, 667 (1930).
(9) E. R. Andrew, *Prog. NMR Spectrosc.*, 8, 1 (1972).
(10) A. C. Wang, A. N. Garroway, and W. M. Ritchey, *Macromolecules*, 14, 832 (1981).
(11) G. E. Meyers, *J. Appl. Polym. Sci.*, 26, 747 (1981).
(12) D. C. VanderHart, W. L. Earl, and A. N. Garroway, *J. Magn. Reson.*, 44, 361 (1981).
(13) J. S. Frye and G. E. Maciel, *J. Magn. Reson.*, 48, 125 (1982).
(14) A. Pines, M. G. Gibby, and J. S. Waugh, *J. Chem. Phys.*, 59, 569 (1973).
(15) D. E. Demco, J. Tegenfeldt, and J. S. Waugh, *Phys. Rev. B*, 11, 4133 (1975).
(16) M. Mehring, *NMR Basic Princ. Prog.*, 11, 112 (1976).
(17) W. T. Dixon, *J. Magn. Reson.*, 44, 220 (1981).
(18) W. T. Dixon, J. Schaefer, M. D. Sefcik, E. D. Stejskal, and R. A. McKay, *J. Magn. Reson.*, 45, 173 (1981).
(19) J. Herzfeld and A. E. Berger, *J. Chem. Phys.*, 73, 6021 (1980).
(20) A. D. English and R. D. Farlee, in progress.
(21) Reference 4 claims the identification of an infrared band at $\sim$1360 cm^{-1} that is thought to be characteristic of $>NCH_2N<$. We do not observe any spectroscopic changes in this region as a function of weathering or depth.
(22) Unpublished results.

Ordered Structure in Block Polymer Solutions. 3. Concentration Dependence of Microdomains in Nonselective Solvents

Mitsuhiro Shibayama, Takeji Hashimoto,* Hirokazu Hasegawa, and Hiromichi Kawai

Department of Polymer Chemistry, Faculty of Engineering, Kyoto University, Kyoto 606, Japan. *Received July 12, 1982*

ABSTRACT: Formation and development of the microdomain structure of a polystyrene–polyisoprene diblock polymer (SI) (having equal block molecular weights) in solutions with nonselective solvents were studied as a function of a wide range of polymer concentration (C) by means of the small-angle X-ray scattering (SAXS) technique with a position-sensitive detector and a high-power X-ray source. The lamellar microdomain with the identity period D starts to develop at concentration greater than 20 wt % polymer for the particular polymer–solvent pair. It was found that there are two regimes in the concentration dependence of D: (i) in the low-concentration regime (less than 70 wt % polymer in this system), which so far has not been studied by any researchers, D increases with increasing C, while (ii) in the high-concentration regime (greater than 70 wt % polymer), D tends to decrease with increasing C, consistent with earlier results reported by Skoulios et al. and Gallot et al. It is proposed that the increase of D with C in the low-concentration regime is due to increasing segregation power between polystyrene and polyisoprene in the presence of neutral solvent with increasing C and that the decrease of D with C in the high-concentration regime is due to a nonequilibrium effect; that is, the system cannot follow equilibrium appropriate for the higher concentrations within a given time scale of experiments. In this regime the average distance between the chemical junction points along the interface is virtually frozen in, and further removal of the solvent accompanied by increasing C simply results in shrinkage of the domain size perpendicular to the interface. The system can attain only "local" equilibrium and its minimum of free energy for a given fixed value of the average distance between the junction points.

I. Introduction

Existence of the ordered structure in block polymer solutions was first reported by Skoulios et al.[1-3] and later by Vanzo.[4] Further systematic but qualitative studies on the structure of the concentrated block polymer solutions have been carried out by French groups (Sadron, Gallot, Skoulios, and co-workers[5,6]) and also by a German group (Hoffmann and co-workers[7]). A good review was given by Gallot.[8]

These earlier studies were mostly concerned with the ordered structure of block polymers in selective solvents, especially with morphological transition of the microdomains (e.g., from spherical to cylindrical domains) and with change of the domain parameters with polymer concentration. In part 1 of this series, we discussed formation of spherical microdomains for a particular block polymer in a selective solvent and variations of its radius, intersphere distance (D_0), and long-range order over a wide range of volume concentration ϕ_p and temperature T.[9] At low ϕ_p, D_0 varies with $\phi_p^{-1/3}$, which can be described in terms of a deswelling effect, while at high ϕ_p, D_0 varies with $\phi_p^{-0.14}$. The low value of the exponent is due to increasing segregation power between the constituent block chains with increasing ϕ_p or to increasing repulsive interaction

0024-9297/83/2216-1427$01.50/0

between polybutadiene block chains emanating from the spherical domains composed of polystyrene block chains. D_0 decreases with T according to $D_0 \sim (1/T)^{\sim 1/3}$, which was proposed to be a consequence of decreasing segregation power with increasing T. We have also proposed that there exist generally two types of structural transitions with variations of T and ϕ_p, i.e., lattice-disordering transition and order-to-disorder transition. In part 2 of this series,[11] we discussed some effects of structural transitions on rheological properties of the solutions.[10]

In contrast to the studies of the microdomain structure in selective solvents, the systematic studies on the domain structure in nonselective solvents commonly good for both block chains are rather limited. This may be partially because scattering contrast between the two coexisting microphases is considerably smaller in the nonselective solvents than in the selective solvents, resulting in much weaker scattering power compared with the scattering power of the systems with nonselective solvents. A pioneering work may be found in the papers by Gallot et al.[12] and Ionescu et al.[13] They found that the lamellar spacing decreases with increasing polymer concentration C over a limited range of the concentration covered by them (typically greater than 60 wt % polymer concentration).

At first glance their results may look reasonable and be interpreted as the *deswelling effect* accompanied by removal of the solvent. However, one would soon recognize the results are puzzling from a viewpoint of increasing *segregation power* with increasing concentration C; that is, the increase of the segregation power with C causes the lamellar spacing increase.

The increase of the lamellar spacing is accompanied by shrinkage of the average distance a between the chemical junction points along the interface (as depicted in Figure 8). If this shrinkage takes place for a given time scale of experiment, the change of D with C should be able to be interpreted from thermodynamic considerations based on the segregation power. Hence in this criterion, D is *thermodynamically controlled.*

On the other hand, if shrinkage does not take place for a given time scale of experiment, further removal of solvent accompanied by an increase in C simply results in shrinkage of the domain size perpendicular to the interface with a fixed value of the distance a, resulting in a decreased value of D. In other words, the system can attain only *local equilibrium*; i.e., the system attains a minimum free energy for a given fixed value of a, and the domain size is *kinetically controlled.*

In order to confirm our idea described above, we studied the domain size over a much wider range of concentration than those covered by the earlier studies.[8,12,13] Our primary objective is focused especially on the domain size for low concentration C, where equilibrium may be relatively easily achieved (i.e., in the thermodynamically controlled region). The change of the domain size with C in the high-concentration regime will be described in detail elsewhere.[25]

As a neutral solvent we chose toluene in this work. The Flory–Huggins interaction parameter χ's of polystyrene and solvent (χ_{PS-S}) and of polyisoprene and solvent (χ_{PI-S}) are, respectively, 0.44 and 0.40 from ref 23, satisfying the criterion of neutral solvent. Here, the molar volume of toluene was used as the reference volume in the definition of the χ parameters.

II. Experimental Method

A styrene–isoprene diblock polymer (SI) was synthesized by sequential living anionic polymerization with *sec*-butyllithium as an initiator and benzene as a solvent. The polymer has a number-average molecular weight of 9.4×10^4 (measured by membrane osmometry) and a weight fraction of styrene monomer of 0.50 (determined by elemental analysis).

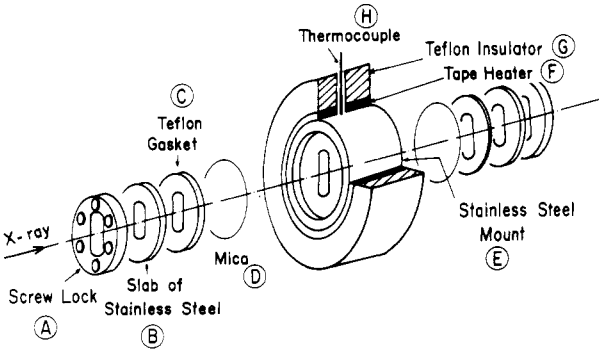

Figure 1. Scattering cell to enclose polymer solution at constant concentration and temperature.

The solution was enclosed in a cell as shown in Figure 1. The thickness of the solution along the incident beam is 2 mm. The cell windows have dimensions of 15-mm height and 4-mm width and are sealed by thin mica or polyester films of about 5-μm thickness which were locked by a screw lock A to a stainless steel mount E. When necessary, the solution was heated by tape heater F, temperature being regulated within an accuracy of ±0.5 °C.

The microdomain structure in the solution was investigated by small-angle X-ray scattering (SAXS) with a linear position-sensitive proportional counter (PSPC), the detailed description being given elsewhere.[15,16] The apparatus utilizes a rotating-anode X-ray generator (RU-a, Rigaku-Denki), operating at 50 kV and 200 mA. Unless otherwise stated, the SAXS results were corrected for absorption, background scattering (air scattering, parasitic scattering, and thermal diffuse scattering), nonuniformity of the detector sensitivity, the collimation errors in both the slit-width and slit-length directions according to a method described elsewhere.[16]

III. Results

Figure 2 shows variations of polymer concentration C (in weight fraction) (a) and SAXS profiles (b) with time during the solvent evaporation process at 33 °C. This experiment was carried out by placing a 9.5 wt % toluene solution in a Petri dish of 9.7-cm diameter, the dish itself being placed in a toluene vapor atmosphere. From time to time the solution was sampled twice, one sample being placed into a weighing bottle for determination of concentration of the solution at time t and the other into the scattering cell for measurement of the SAXS profile at that concentration at t. The concentration of a given solution was measured by weighing the solution before and after solvent evaporation, the solution being dried at 50 °C in a vacuum oven until it showed a constant weight. The scattering profile at a given concentration was measured at 25 °C about 0.5 h after the solution was enclosed in the cell. The measuring time was typically 1000–2000 s. There was no trace of solvent leakage from the cell.

As solvent is evaporated, concentration sigmoidally increases with time as shown in Figure 2a. Figure 2b shows development of microdomain structure at each point A–E as observed by SAXS profiles, the concentration of A–E being 19, 27, 37, 45, and 70 wt % (see Figure 2). The scattering maximum appears at concentrations greater than about 27 wt %, and the intensity increases with concentration, indicating that the microdomain structure starts to develop at about 27 wt % and segregation of the block chains in the respective microdomains further progresses with increasing concentration.

Figure 3 shows quantitative displays of the smeared scattering profiles at various concentrations at room temperature, where s is defined as

$$s = (2 \sin \theta)/\lambda \quad (1)$$

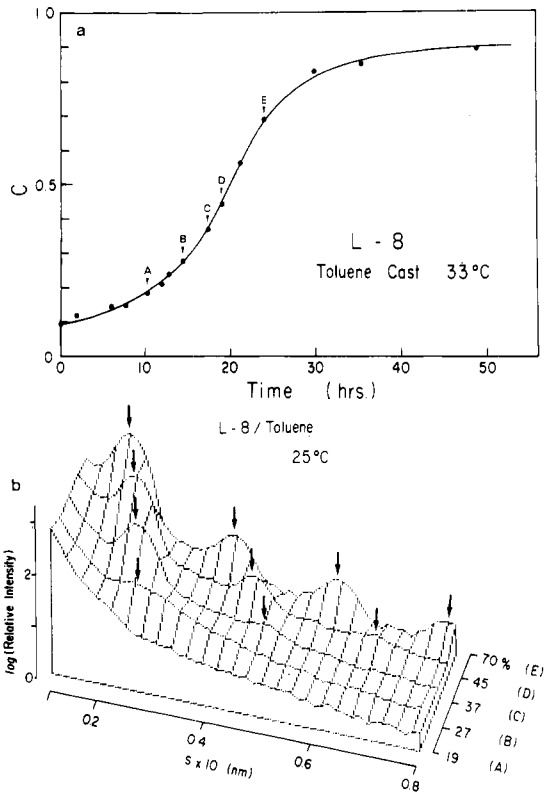

Figure 2. (a) Variation of concentration C of toluene solution of the block polymer with time during the solvent evaporation process at 33 °C. Initial concentration is 9.5 wt %. (b) Scattering intensity profiles taken at 25 °C at various concentrations A–E in (a).

2θ is the scattering angle and λ is the wavelength of the X-rays (0.154 nm). At low concentrations, $C < 0.2$, the scattering intensity is very weak and intensity continuously decreases with s. The scattering maximum appears at concentrations greater than 20 wt %. With a further increase of the concentration, the scattered intensity increases, and the higher order scattering maxima appear at the peak positions of 1:2:3:4:... relative to the peak position of the first-order maximum. The results indicate that the lamellar microdomains are developed in the solutions at concentrations greater than 20 wt % and that the segregation continuously progresses with increasing concentration.

The Bragg spacing D was estimated from the peak position s_n or $2\theta_n$ of the nth-order scattering maximum

$$s_n = (2 \sin \theta_n)/\lambda = n/D \tag{2}$$

the results of which are shown in Figure 6. The spacing D was estimated from the peak position of the desmeared scattering profile (the data being shown by solid circles), corrected both for slit-length and slit-width smearings. The data shown by solid triangles were obtained from the peak position of the Lorentz-corrected, desmeared curve (i.e., from the peak position of the profile $s^2I(s)$, where $I(s)$ is the desmeared curve). Figure 4 shows a typical desmeared profile obtained for the solution with 70 wt % concentration. It is seen clearly by comparing Figures 3 and 4 that the desmeared profile shows much sharper intensity variation with 2θ or s than the smeared profile. However, the peak positions themselves hardly shift with the desmearing for the slit-weighting functions employed in these studies.

Figure 5 shows the smeared scattered intensity distributions for the films cast from toluene (as cast) and subsequently annealed at 120 °C under vacuum for 8 h (annealed). The incident X-ray beam is irradiated parallel to the film surface (edge radiation) and the scattered X-ray beam was detected along the direction normal to the film surface. As is well-known, the lamellar microdomains in the solvent-cast films tend to orient with the boundaries parallel to the film surface.[17,18] If the slit-shaped focus image of the X-ray beam is aligned parallel to the film surface as employed in this work, the slit-height smearing effect should be negligible, and the measured profiles are affected only by slit-width smearing, which is not of great importance in these studies. However, it is important to note that the peak shifts to smaller angles and hence the lamellar identity period increases from 49.2 nm to 52.7 nm with the annealing. This reflects clearly nonequilibrium aspects of domain formation, which will be described in detail in the next section (section IV-2).

IV. Discussion

1. Concentration Dependence. Figure 6 shows the variation of the lamellar identity period D with polymer concentration C. Periodic segmental density fluctuations typical for the lamellar microdomain start to develop at C greater than about 0.2. The domain spacing D gradually *increases* with concentration from 30 nm to 50 nm in the concentration range up to $C \simeq 0.7$. It should be noted that D increases with C despite increasing *deswelling*, which is best interpreted as a consequence of increasing segregation power (or repulsive interactions) between polystyrene (PS) and polyisoprene (PI) block chains with increasing C in the presence of the neutral solvent as discussed in detail below. One should also note that the D value of the bulk polymer does not come to a value extrapolated to zero solvent concentration ($C = 1$), the value for the as-cast bulk specimen being significantly smaller than the extrapolated value. This is indicative of the tendency of *decreasing D with increasing C*, which is consistent with previous results reported by Skoulios et al.[13] and Gallot et al.[8,12] We speculate that this is due to a nonequilibrium effect in the solvent evaporation process as described in detail below.

It should be noted that D values estimated from the Lorentz-corrected profiles are slightly smaller than those estimated from the Lorentz-uncorrected profiles. However, the correction does not alter the relative concentration dependence of the domain spacing.

One can estimate the concentration dependence of (i) S/N, the average interfacial area occupied by a single block chain, and (ii) d_{PS} and d_{PI}, the thickness of polystyrene and polyisoprene lamellae, respectively, from the concentration dependence of D based on the equations[19]

$$\frac{d_K}{D} = \frac{w_K C/\rho_K + \alpha_K(1 - C)/\rho_S}{C[w_{PS}/\rho_{PS} + (1 - w_{PS})/\rho_{PI}] + (1 - C)/\rho_S} \tag{3}$$

$$K = PS \text{ or } PI$$

$$\frac{S}{N} = \frac{2M}{DCN_A}\{C[w_{PS}/\rho_{PS} + (1 - w_{PS})/\rho_{PI}] + (1 - C)/\rho_S\} \tag{4}$$

where w_K is the weight fraction of K-block chain (K = PS or PI) in the block polymer, ρ_K and ρ_S are the mass densities of the K polymer and solvent, respectively, α_K is the partition fraction of solvent to the domain composed of K-block polymer, M is the total molecular weight of the block polymer, and N_A is Avogadro's number.

Equations 3 and 4 assume a complete segregation of block chains such that PS (PI) domains are composed only of PS (PI) segments and solvent. The assumption is only good as a first approximation but may suffice to predict general tendencies of concentration dependence of d_K and

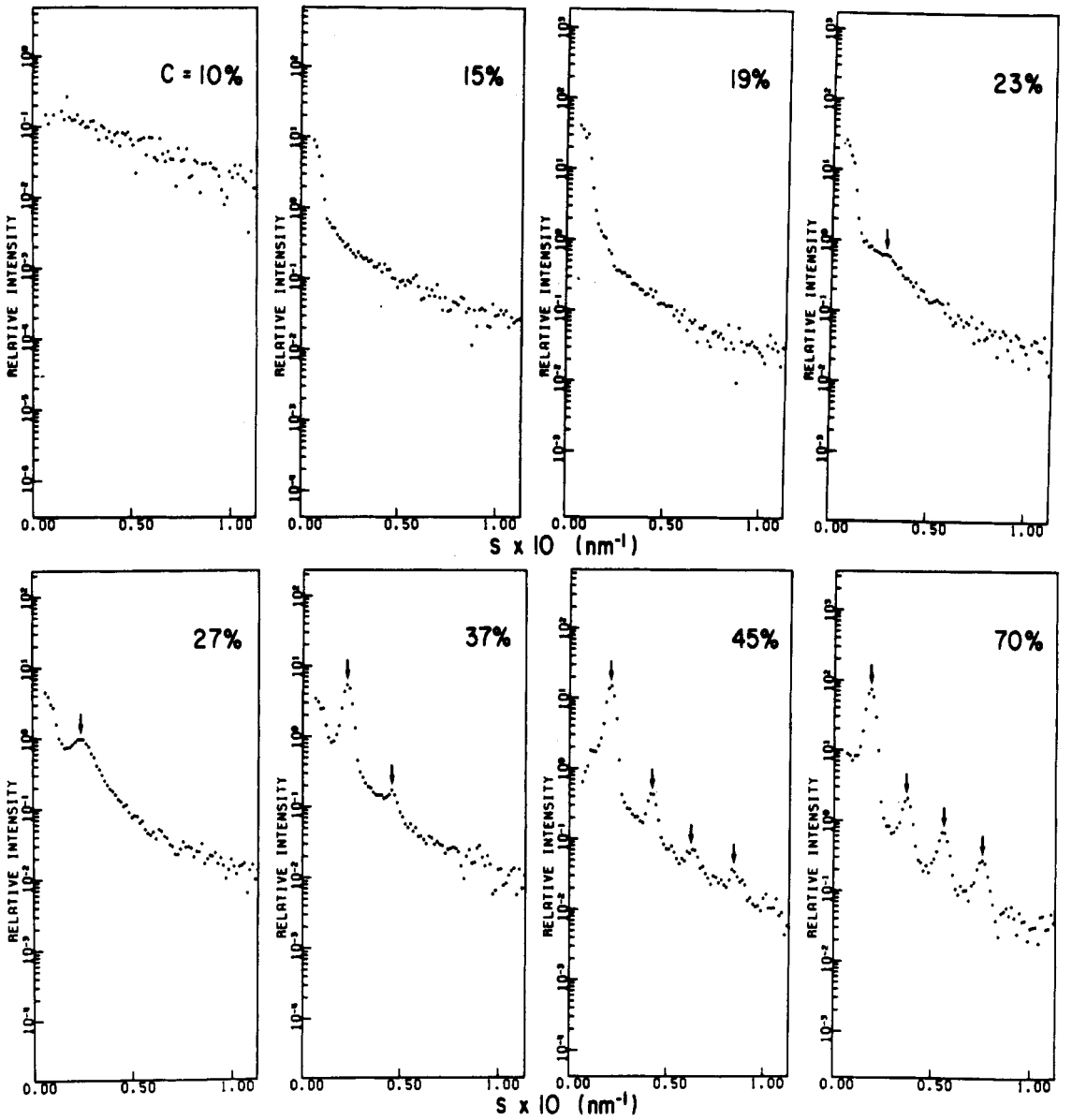

Figure 3. Smeared SAXS intensity profiles at various concentrations C at room temperature. $s = (2 \sin \theta)/\lambda$, 2θ and λ being the scattering angle and the wavelength of the X-rays, respectively.

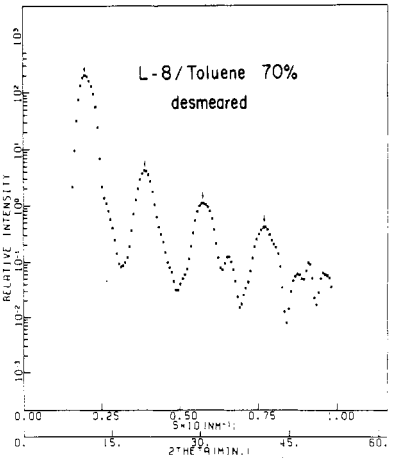

Figure 4. Desmeared SAXS intensity profile for 70 wt % solution at 25 °C.

$(S/N)^{1/2}$. The results shown in Figure 7 are obtained by assuming equal partition of solvent into each domain, i.e., $\alpha_{PS} = \alpha_{PI}$, which is a good approximation. It is of particular interest to note that the value $(S/N)^{1/2}$, the average distance between neighboring chemical junction points along the interface, decreases with C. That is, the chemical junction points come close to each other along the interface with increasing C. This involves perturbation of the block chains along the direction normal to the interface, the process of which, in turn, involves increasing the domain size and decreasing the interfacial area and consequently decreasing the surface-to-volume ratio. The repulsive interaction between PS and PI block chains increases with C, which, however, is stabilized by this mechanism of decreasing the surface-to-volume ratio.

Figure 8 shows a model describing the concentration dependence of D. In the strong segregation limit, the block chains segregate themselves into their respective domains as shown in Figure 8b, giving rise to the spatial segmental density profiles $\tilde{\rho}_K$ (K = A or B) as shown in Figure 8a. Mixing of A and B segments may occur only in the interfacial region (domain-boundary region) having the "characteristic interfacial thickness" t_1, which was defined as $(2\pi)^{1/2}\sigma$ in ref 20. Since polymeric liquids are highly incompressible, the system has to satisfy the demand of "uniform filling of space" with segments in the equilibrium state, i.e., $\tilde{\rho}_A + \tilde{\rho}_B$ being constant everywhere in the domain space. Owing to the repulsive interaction of the constituent block chains,[21,22] the chains tend to be perturbed normal

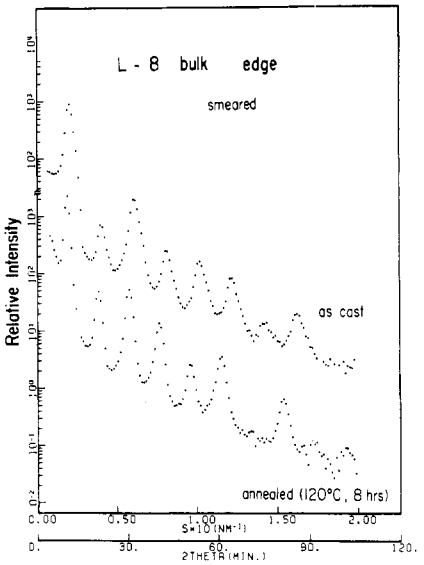

Figure 5. Smeared SAXS intensity profiles for bulk films taken with edge radiation: (top profile) as-cast films; (bottom profile) films annealed at 120 °C under vacuum for 8 h.

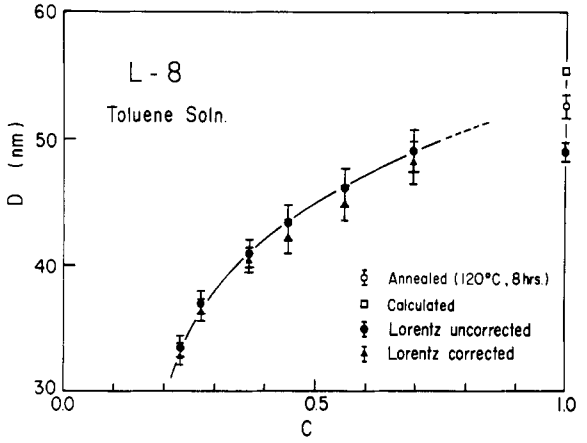

Figure 6. Concentration dependence of the identity period D of the lamellar microdomains developed in solution. The solid circles and triangles are obtained, respectively, from the Lorentz-uncorrected and Lorentz-corrected scattering profiles. The open circle corresponds to D for the bulk films after the as-cast films are annealed at 120 °C for 8 h. The open square is the equilibrium domain spacing at 25 °C calculated from Helfand–Wasserman theory.

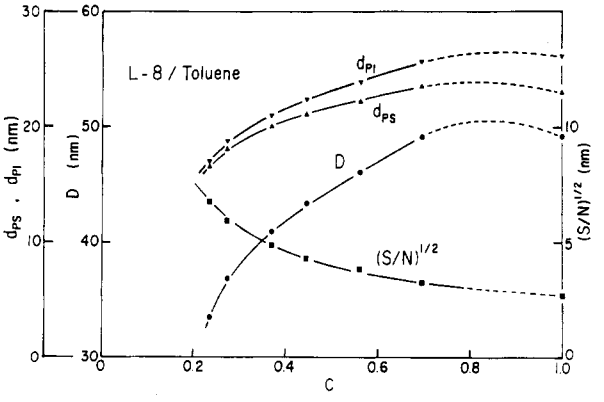

Figure 7. Variations of domain identity period D, thicknesses of polyisoprene lamellae (d_{PI}) and polystyrene lamellae (d_{PS}), and square root of average interfacial area occupied by a block chain $(S/N)^{1/2}$ with C.

to the interface. In order to minimize free energy of the domain system under the constraint of *uniform filling of space*, spatial segmental density variation of a given block

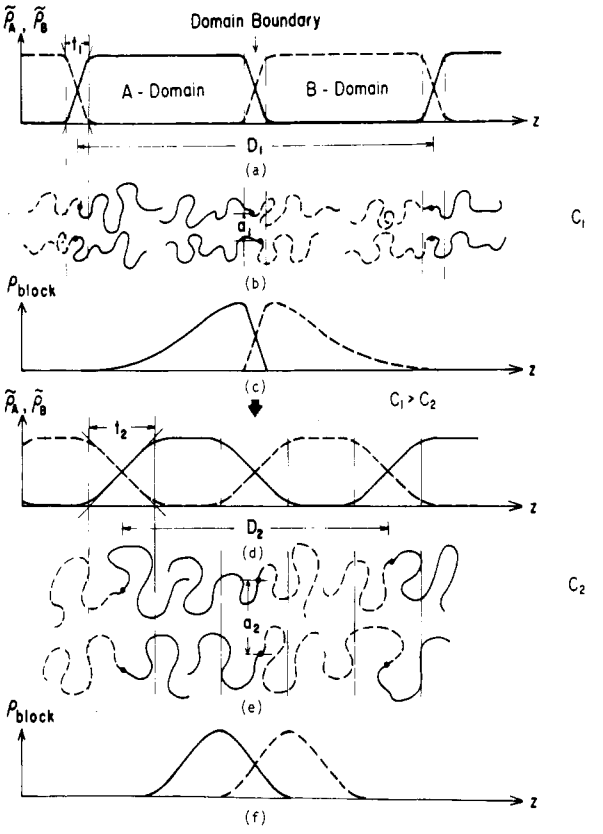

Figure 8. Schematic diagram showing concentration dependence of domain size (from D_1 to D_2), average nearest-neighbor distance between the chemical junction points along the interface (from a_1 to a_2), and spatial segmental density profile of a given block chain. The concentration C_1 is greater than C_2.

chain should be skewed as shown in Figure 8c. That is, the skewed segmental density distribution raises the conformational free energy of the *confined chains* but lowers the mixing free energy of the unlike segments. Thus the skewness is balanced by the two opposing physical factors and is primarily determined by the segregation power. The greater the effective thermodynamic interaction parameter χ_{eff} between the constituent block chains in the presence of the solvent, the larger the skewness.

When the concentration is lowered, the repulsive interaction of the chains decreases. Consequently, A-block chains tend to have some walks in B domains, resulting in a smaller end-to-end distance and hence in smaller domain spacing D_2 and in thicker domain-boundary thickness t_2 as shown in Figure 8d. Since χ_{eff} decreases as concentration is lowered, the segmental density distribution for a given chain becomes a more symmetric Gaussian-type distribution (Figure 8f). It is important to note that the decrease of the domain size is simply adjusted by an increase of the distance from a_1 to a_2 between the chemical junction points along the interface (Figure 8e). Thus an increase of the spacing D with increasing C is a consequence of the segregation power outweighing the deswelling effect. The *lamellar thickening*, which involves loss of conformational entropy, is stabilized by decreasing the surface-to-volume ratio, i.e., by decreasing mixing free energy of the unlike segments.

Figure 9a shows comparisons of theoretical and experimental concentration dependence of D. The experimental values (uncorrected by the Lorentz factor) are shown by solid circles, while the theoretical results by Meier (M) and Noolandi and Hong (N–H)[23] are drawn, respectively, by dash–dot and broken lines. Meier's result was obtained by replacing χ by $\chi\phi_P$ in the theory of the lamellar mi-

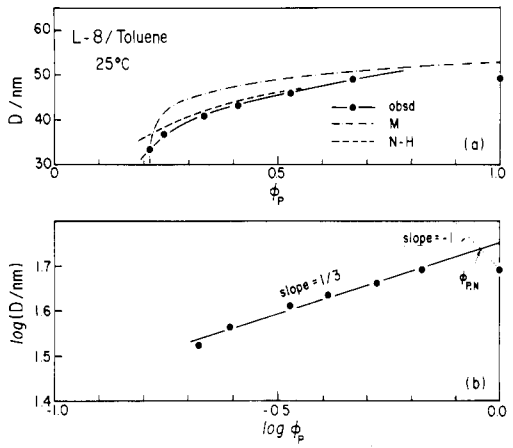

Figure 9. (a) Comparison between the experimental and theoretical concentration dependence of the lamellar spacing D. The experimental data are shown by solid circles, while the dash–dot line and broken line are, respectively, the calculated results from the theories of Meier (M) and Noolandi and Hong (N–H). (b) Concentration dependence of the lamellar spacing D. The experimental data (solid circles) closely fit $D \sim \phi_p^{1/3}$ (solid line), where ϕ_p is the volume fraction of polymer. The dotted line is the change of spacing D with decreasing ϕ_p according to "one-dimensional swelling" of the bulk films ($D \sim \phi_p^{-1}$; see text).

crodomain for the bulk block polymer,[26] where ϕ_P is the volume fraction of polymer in the solution and χ is the χ parameter between polystyrene and polyisoprene block chains in bulk. The same molecular parameters as described in ref 20 were used for the calculations. Noolandi and Hong's result was obtained by using the following parameters: $\chi = 0.075$, $\chi_{PS-S} = 0.44$, $\chi_{PI-S} = 0.40$. The average Kuhn statistical segment length is 0.72 nm.

Good agreements between the experimental and theoretical results were obtained except for the behavior at high concentrations. The equilibrium theories predict that the D values continue to increase, while the experimental results indicate that the D values tend to decrease at $\phi_P \gtrsim 0.7$ to result in the D value at $\phi_P = 1.0$. That is, the agreements between the theories and experiments are fine in the *low-concentration regime* where the microdomains are controlled by the segregation power and are *thermodynamically controlled*. However, no agreements are obtained in the *high-concentration regime*, which may be quite reasonable because the *kinetic effect* controls the domain size in this regime.

Figure 9b shows the experimental concentration dependence of D in the double-logarithmic plot. In the low-concentration regime, the data points fall on a straight solid line with slope $^1/_3$, thus leading to

$$D \sim \phi_P^{1/3} \tag{5}$$

It may be apparent that the behavior in the high-concentration regime ($\phi_P \gtrsim 0.7$) deviates from eq 5, which will be described in the next section. The dependence of D on temperature and molecular weight was partially described in ref 14a and will be fully reported elsewhere.[14b]

2. Nonequilibrium Aspects of Domain Formation in Lamellar Microdomains. In this section we discuss the concentration dependence of the lamellar spacing in the high-concentration regime, $\phi_P \gtrsim 0.7$ for this particular system.

The most important experimental evidence in this concentration regime is that the D value of the bulk polymer (as-cast bulk films) is significantly *smaller* than the value extrapolated to $C = 1$ from the lower concentrations as shown in Figures 6, 7, and 9. Figure 9 shows the extrapolated value of D being 58.9 nm, much larger than the value 49.2 nm for the as-cast bulk films. In the preceding section it is pointed out that the growth of domains (lamellar thickening) with concentration involves (i) perturbations of block chains normal to the interface and (ii) displacement of the chemical junction points along the interface (*two-dimensional shrinkage*) to reduce the average distance between them (see Figure 8). As the concentration is raised, this process should be hindered because of one of the following two mechanisms or a combination of the two: as the concentration becomes high, (i) the glass transition temperature reaches the ambient temperature and/or (ii) the modulus of the whole system becomes high so that the cooperative deformation of each *grain* (within which the orientation of the microdomains is coherent) requires a prolonged equilibration time. The increase of the lamellar spacing involves deformation of the grain such that the dimension of the grain normal to the lamellar interfaces should expand but its lateral dimensions may contract. The relaxation time associated with cooperative deformation of each grain may be characterized as *grain-boundary relaxation* and be a function of modulus and size of the grain and of viscosity and size of the grain boundary.

It follows eventually that within a given time scale of the solvent evaporation the chemical junction points cannot be rearranged to a state appropriate for an equilibrium at the concentration. Thus at the very high concentration regime, the distance between the neighboring chemical junction points (a) or the average number of block chains per unit interfacial area (N/S) is essentially fixed. Further evaporation of solvent results in a decrease of the domain spacing merely by a deswelling effect. Thus in this regime the domain spacing is *kinetically controlled* but not *thermodynamically controlled*. At lower concentrations, the rate of the lateral displacement may be much faster than the solvent evaporation rate. Consequently, the nonequilibrium effect is less significant, and the domain size is thermodynamically controlled.

When the as-cast bulk films are annealed at 120 °C under vacuum for 8 h (a temperature higher than the glass transition temperature of PS), the spacing increases from 49.2 nm to 52.7 nm as shown in Figure 6. This is merely a consequence of the system approaching equilibrium. When the temperature is lowered from 120 °C to room temperature, the thermodynamically-controlled domain spacing should increase slightly because of increasing segregation power with lowering temperature. However, the domain spacing is again controlled by the *kinetic effect* when the temperature is lower than the glass transition temperature of PS domains. Thus the domain spacing for the annealed specimens is the one relevant to equilibrium at ca. 100 °C but not at room temperature. The spacing shown by an open square in Figure 6 is the *equilibrium* spacing at 25 °C calculated from the Helfand–Wasserman theory.[24] Thus the problem raised in the introductory section in connection with earlier results reported by French groups may be basically solved by the nonequilibrium effect encountered in the solvent evaporation process.

The dotted line in Figure 9b represents a hypothetical concentration dependence of D in which the domain spacing increases with decreasing ϕ_P by "one-dimensional" swelling, i.e., the swelling normal to the interfaces with a fixed distance a (average distance between the neighboring chemical junction points) or N/S (number of the block chains per unit interfacial area)

$$D \sim \phi_P^{-1} \tag{6}$$

In the case when a decreases with increasing concentration

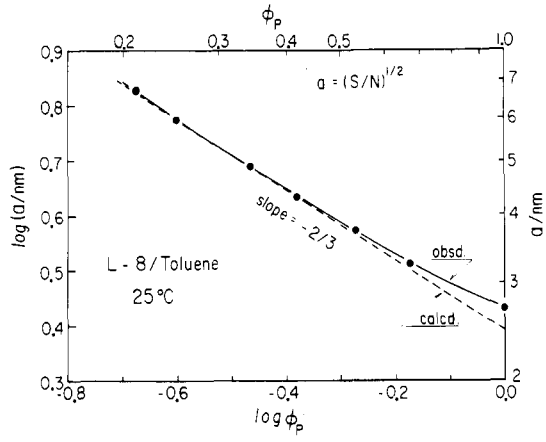

Figure 10. Concentration dependence of average nearest-neighbor distance a between the chemical junction points along the interface. The solid circles and solid line are estimated from eq 4 and the broken line is estimated from eq 9.

at $\phi_P < \phi_{P,N}$ according to a scheme that gives rise to $D \sim \phi_P^{1/3}$ but remains constant at $\phi_P > \phi_{P,N}$, the variation of D with ϕ_P is such that at $\phi_P \leq \phi_{P,N}$ it is described by the solid straight line and at $\phi_P > \phi_{P,N}$ by the dotted line. $\phi_{P,N}$ is the crossover point of the solid and dotted lines in Figure 9b.

D and N/S are related to each other by

$$D = 2(N/S)\bar{v} \tag{7}$$

where $\bar{v}$ is the volume occupied by a block chain in the presence of solvent. Since

$$\bar{v} \sim \phi_P^{-1} \tag{8}$$

and $D \sim \phi_P^{1/3}$ from the evidence shown in Figure 9b, we can predict a should vary with ϕ_P according to

$$a \equiv (S/N)^{1/2} \sim \phi_P^{-2/3} \tag{9}$$

The value of N/S or a can also be estimated from eq 4 by knowing D and the concentration C.

Figure 10 shows the variation of a with ϕ_P as predicted from eq 9 (broken line) and from eq 4 (solid circles and solid line). The decrease of a with increasing ϕ_P tends to be slowed down at high concentrations $\phi_P \gtrsim 0.7$, primarily due to the nonequilibrium effect described above.

3. Some Comparisons with Previous Works. Pioneering works had been carried out by Gallot et al.[12] and Skoulios et al.[13] at a relatively high-concentration limit ($C \geq 0.6$). They reported that the domain spacing D decreases with increasing C at $C > 0.6$ (see, for example, Figure 5 of ref 12 and Figure 1 of ref 13). We also confirmed this tendency *in the high-concentration regime* ($\phi_P \gtrsim 0.7$ for this particular system). In light of our present studies we may propose that in the concentration regime covered by them or in the high-concentration regime in this work, the domain spacing is kinetically controlled rather than thermodynamically controlled. We expect and presented experimental evidence that if the concentration is further lowered, the systems reach the regime where the domain size is controlled by thermodynamics and D should increase with C or ϕ_P.

Finally, they claimed that the partition fraction of solvent to each domain is not identical but toluene is a slightly better solvent for PS than for PI. Although we did not discuss the details of the partition, we agree with their conclusions. From the variation of the relative peak heights of the SAXS with concentration, one can estimate the variation of volume fraction of each domain with concentration,[17] which, in turn, yields information on the partition fraction. Apparently, the relative peak heights of the SAXS for the bulk specimens (Figure 5) are different from those for the solution (e.g., Figure 4 for $C = 0.7$), indicating that the partition fractions of the solvent to PS and PI are slightly different.

Acknowledgment. We are grateful to Dr. J. Noolandi, Xerox Research Centre of Canada, and Dr. D. J. Meier, Midland Molecular Institute, for sending the theoretical values of D for L-8 in toluene solution (Figure 9). We have benefited from helpful discussions with Dr. Meier. A part of this work is supported by a Grant-in-Aid for Special Project Research (No. 5711903) from the Ministry of Education, Science and Culture, Japan, and by Grant No. 56490013.

Registry No. Styrene–isoprene copolymer, 25038-32-8.

References and Notes

(1) Skoulios, A.; Finaz, G.; Parrod, J. *C. R. Hebd. Seances Sci.* **1960**, *251*, 739.
(2) Skoulios, A.; Finaz, G. *C. R. Hebd. Seances Acad. Sci.* **1961**, *252*, 3467.
(3) Finaz, G.; Skoulios, A.; Sadron, C. *C. R. Hebd. Seances Acad. Sci.* **1961**, *253*, 265.
(4) Vanzo, E. *J. Polym. Sci., Part A-1* **1966**, *4*, 1727.
(5) Sadron, C.; Gallot, B. *Makromol. Chem.* **1973**, *164*, 301.
(6) Skoulios, A. In "Block and Graft Copolymers"; Burke, J. J., Weiss, V., Eds.; Syracuse University Press: Syracuse, NY, 1973.
(7) Hoffmann, M.; Kämpf, G.; Krömer, H.; Pampus, G. *Adv. Chem. Ser.* **1971**, *No. 99*, 351.
(8) Gallot, B. *Adv. Polym. Sci.* **1978**, *29*, 87.
(9) Shibayama, M.; Hashimoto, T.; Kawai, H. *Macromolecules* **1983**, *16*, 16 (part 1 of this series).
(10) Watanabe, H.; Kotaka, T.; Hashimoto, T.; Shibayama, M.; Kawai, H. *J. Rheol.* **1982**, *26* (2), 153.
(11) Hashimoto, T.; Shibayama, M.; Kawai, H.; Watanabe, H.; Kotaka, T. *Macromolecules* **1983**, *16*, 361 (part 2 of this series).
(12) Douy, A.; Mayer, R.; Rossi, J.; Gallot, B. *Mol. Cryst. Liq. Cryst.* **1969**, *7*, 103.
(13) Ionescu, M.-L.; Skoulios, A. *Makromol. Chem.* **1976**, *177*, 257.
(14) (a) Hashimoto, T.; Shibayama, M.; Kawai, H. *Polym. Prepr., Am. Chem. Soc., Div. Polym. Chem.* **1982**, *23* (1), 21. (b) Hashimoto, T.; Shibayama, M.; Kawai, H. *Macromolecules* **1983**, *16*, 1093 (part 4 of this series).
(15) Hashimoto, T.; Suehiro, S.; Shibayama, M.; Saijo, K.; Kawai, H. *Polym. J.* **1981**, *13*, 501.
(16) Fujimura, M.; Hashimoto, T.; Kawai, H. *Mem. Fac. Eng. Kyoto Univ.* **1981**, *43* (2), 224.
(17) Hashimoto, T.; Nagatoshi, K.; Todo, A.; Hasegawa, H.; Kawai, H. *Macromolecules* **1974**, *7*, 364.
(18) Hashimoto, T.; Todo, A.; Itoi, H.; Kawai, H. *Macromolecules* **1977**, *10*, 377.
(19) Sadron, C.; Gallot, B. *Makromol. Chem.* **1973**, *164*, 301.
(20) Hashimoto, T.; Shibayama, M.; Kawai, H. *Macromolecules* **1980**, *13*, 1237.
(21) Meier, D. J. *J. Polym. Sci., Part C* **1969**, *26*, 81.
(22) Helfand, E. *Macromolecules* **1975**, *8*, 552.
(23) Noolandi, J.; Hong, K.-M. *Ferroelectrics* **1980**, *30*, 117.
(24) Helfand, E.; Wasserman, Z. R. *Macromolecules* **1976**, *9*, 879.
(25) Shibayama, M.; Hashimoto, T.; Kawai, H. *Macromolecules* **1983**, *16*, 1434 (part 5 of this series).
(26) Meier, D. J. *Prepr. Polym. Colloq., Soc. Polym. Sci., Jpn.* **1977**, 83.